Video Article

Dissipative Microgravimetry to Study the Binding Dynamics of the Phospholipid Binding Protein Annexin A2 to Solid-supported Lipid Bilayers Using a Quartz Resonator

Anna Livia L. Matos*[1,3], David Grill*[1,3], Sergej Kudruk[1,3], Nicole Heitzig[1,3], Hans-Joachim Galla[2,3], Volker Gerke[1,3], Ursula Rescher[1,3]

[1]Institute of Medical Biochemistry, Center for Molecular Biology of Inflammation, University of Münster

[2]Institute of Biochemistry, University of Münster

[3]Cluster of Excellence 'Cells in Motion', University of Münster

*These authors contributed equally

Correspondence to: Ursula Rescher at rescher@uni-muenster.de

URL: https://www.jove.com/video/58224
DOI: doi:10.3791/58224

Keywords: Biochemistry, Issue 141, Microbalance, solid-supported bilayer, phospholipid microdomains, cholesterol, annexins, cooperativity, binding dynamics, viscoelastic properties

Date Published: 11/1/2018

Citation: Matos, A.L., Grill, D., Kudruk, S., Heitzig, N., Galla, H.J., Gerke, V., Rescher, U. Dissipative Microgravimetry to Study the Binding Dynamics of the Phospholipid Binding Protein Annexin A2 to Solid-supported Lipid Bilayers Using a Quartz Resonator. *J. Vis. Exp.* (141), e58224, doi:10.3791/58224 (2018).

Abstract

The dissipative quartz crystal microbalance technique is a simple and label-free approach to measure simultaneously the mass uptake and viscoelastic properties of the absorbed/immobilized mass on sensor surfaces, allowing the measurements of the interaction of proteins with solid-supported surfaces, such as lipid bilayers, in real-time and with a high sensitivity. Annexins are a highly conserved group of phospholipid-binding proteins that interact reversibly with the negatively charged headgroups *via* the coordination of calcium ions. Here, we describe a protocol that was employed to quantitatively analyze the binding of annexin A2 (AnxA2) to planar lipid bilayers prepared on the surface of a quartz sensor. This protocol is optimized to obtain robust and reproducible data and includes a detailed step-by-step description. The method can be applied to other membrane-binding proteins and bilayer compositions.

Video Link

The video component of this article can be found at https://www.jove.com/video/58224/

Introduction

Cellular membranes are highly dynamic and complex structures. The compound mixture of membrane lipids, together with peripherally and/or integrally associated membrane proteins, assemble to form microdomains. The coordinated tempo-spatial organization of these membrane microdomains is involved in key physiological processes[1]. Membrane microdomain dynamics are driven by the interplay of membrane lipids, as well as by the ability of peripheral membrane proteins to recognize and interact with lipids enriched in the microdomains. The recruitment of the proteins to the specific lipids is often achieved *via* lipid-recognition modules, such as the pleckstrin homology (PH) or the C2 domains[2,3]. Biophysical analytical methods using model membranes are key to understanding the fundamental principles governing these processes at the molecular level.

Annexins, a large multigene-family, are well-known for their ability to bind to negatively charged membrane lipids, predominantly phosphatidylserine (PS), in a Ca^{2+}-controlled manner[2]. The second hallmark of the annexin family is the presence of a conserved structural segment, the annexin repeat, that is present four or eight times and harbors the Ca^{2+}- and phospholipid-binding sites[4]. The Ca^{2+}-dependent lipid interaction places the annexins in a perfect position to sense and convey Ca^{2+}-mediated signaling to target membranes. Consistently, annexins are able to induce the formation of microdomains enriched in cholesterol, phosphatidylinositol-4,5-bisphosphate ($PI(4,5)P_2$), and PS, both in cellular and/or artificial membrane systems[5]. This protocol describes an approach to analyze the annexin-membrane interaction using a Quartz Crystal Microbalance Dissipation (QCM-D)[6,7,8].

The basic component in this microbalance is an oscillating crystal that serves as the sensor surface. The adsorption and/or binding of molecules to the sensor surface decreases the resonance frequency (f) proportional to the increase in mass. If the surface is evenly coated with a film, the binding of additional substances may interfere with the structural integrity of this layer, and such changes in viscoelasticity (the energy dissipation factor D) can be additionally monitored. This is a widespread technique to study the interaction of proteins with lipid bilayers. In this approach, lipid vesicles are absorbed onto the appropriately coated sensor surface. Lipid bilayer formation is favorable on silica-based materials[9,10], as vesicles often do not rupture on other hydrophilic surfaces, such as gold[11] oxidized after UV-ozone exposure, TiO_2[12], or Al_2O_3[13]. The rupture of the coalescing vesicles releases the aqueous phase, leading to characteristic changes in mass and dissipation. The generation of solid-supported bilayers (SLB) by vesicle fusion is simple and robust and can be used to generate complex models that mimic cellular membranes.

Dissipative quartz crystal microbalance is a label-free and sensitive technique. A major advantage is the possibility to coat any material that generates a sufficiently thin film onto the surface, thus providing a broad range of applications in diverse research areas. The protein-membrane interaction is observed in real-time, and the results can be analyzed directly. The same sensor surface can be used in subsequent measurements (after performing a minimal cleaning as described in this protocol), thus allowing for accurate internal controls and a comparability between analytes.

Protocol

NOTE: Buffers should be filtered using a 0.22-µm filter and degassed by a vacuum for 1 h.

1. Lipid Vesicle Preparation

1. Use 2-mL glass tubes. Dissolve each lipid, 1,2-dioleoyl-sn-glycero-3-phosphocholine (DOPC), 1-palmitoyl-2-oleoyl-sn-glycero-3-phosphocholine (POPC), 1-palmitoyl-2-oleoyl-sn-glycero-3-phospho-L-serine (POPS), and cholesterol (Chol), in a mixture of chloroform/methanol (50:50 v/v) to prepare a clear 5 mM lipid solution. Dissolve 1,2-dioleoyl-sn-glycero-3-phospho-(1'-myo-inositol-4',5'-bisphosphate) ($PI(4,5)P_2$) in a mixture of chloroform/methanol/water (20:9:1 v/v).
2. Combine the dissolved lipids in the desired molar ratio of POPC/POPS (80/20), POPC/$PI(4,5)P_2$ (95/5), POPC/POPS/Chol (60/20/20), POPC/POPS/$PI(4,5)P_2$/Chol (60/17/3/20), and POPC/DOPC/POPS/$PI(4,5)P_2$/Chol (37/20/20/3/20) (**Table 1**) in 10-mL glass tubes.
   NOTE: The final amount of total lipid is 500 µg.
3. Evaporate the organic solvents using a dry stream of nitrogen. Leave the lipid mixture on a high vacuum (lyophilization) system for 3 h to remove any residual traces of the solvents.
   NOTE: This results in a dry clear film.
4. Resuspend the lipid film in 1 mL of citrate buffer (10 mM trisodium-citrate, 150 mM NaCl, pH 4.6). Incubate the lipid suspension at 60 °C (this temperature is around 10 °C above the phase transition temperature of the highest melting lipid in the mixture) for 30 min in a water bath, and vortex it vigorously every 5 min.
   NOTE: This results in the formation of large, multilamellar vesicles (MLVs). Keep the suspension above the transition temperature.
5. Preheat the extruder (at 60 °C in this case) equipped with a 50-nm diameter pore-size polycarbonate membrane above the transition temperature (which is 40 - 50 °C here) for 30 min.
6. Load the MLV suspension into the preheated extruder and gently pass the mixture 31x through the polycarbonate membrane to form small unilamellar vesicles (SUVs)[14]. Keep the temperature above the transition temperature.
7. Transfer the SUV suspension to a 2 mL plastic reaction vessel and add the citrate buffer (see step 1.4) to bring the final volume to 2 mL.
   NOTE: This will yield a final lipid concentration of 250 µg/mL.

2. Handling the Quartz Sensors

NOTE: Always handle the quartz sensors with a tweezer.

1. Incubate four sensors inserted in a polytetrafluoroethylene holder in a 2% SDS solution for ≥ 30 min. Wash them extensively with ultra-pure water to completely remove the SDS and let them dry using a stream of dry argon or nitrogen.
2. Use a plasma-cleaning system to completely remove any contaminants. Insert the dry sensors in the plasma-cleaning chamber, evacuate the chamber, and flush it 3x with oxygen. Turn the plasma cleaner on. Use the following process parameters: 1×10^{-4} Torr pressure, high radio frequency (RF) power, and 10 min of process time. Turn off the machine and take out the sensors.

3. Microbalance Operation

NOTE: A microbalance system with four temperature-controlled flow chambers in a parallel configuration, connected to a peristaltic pump and set to a flow rate of 80 µL/min, was used. In the open flow mode, the buffer was pumped from the feeder reservoir into the receiving tank. In the loop mode, the receiving tank was connected with the feeder reservoir to generate a closed loop. The temperature was set to 20 °C.

1. Carefully dock the plasma-cleaned sensors into the 4 flow chambers, using tweezers. Avoid any pressure on or torsion of the chambers and the tubes that might cause leaking.
2. Flush the system with citrate buffer (10 mM trisodium-citrate, 150 mM NaCl, pH 4.6) in the open-flow mode for 10 min.
   NOTE: This requires exactly 3.2 mL of buffer, but it is advisable to use an excess of buffer (10 mL).
3. Launch the program. Start recording any changes in the frequency and dissipation of the first fundamental tone (*n* = 1st) and overtones (n = 3rd - 13th) using the software, until the frequency and dissipation baselines are stable (this will take around 40 - 60 min).
   NOTE: Frequency noise levels (peak-to-peak) should be lower than 0.5 Hz and, for the dissipation, lower than $0.1 \cdot 10^{-6}$, with a maximal drift (in aqueous solution) of 1 Hz/h in frequency and $0.3 \cdot 10^{-6}$/h in dissipation.
4. When the baselines are stable, apply the SUV suspension in citrate buffer (2 mL in a small tube). Using a reaction vessel, remove 1.5 mL of the dead volume. Then close the system in the loop-flow mode. Record the frequency/dissipation shift for another 10 minutes.
   NOTE: During this time, the vesicles will spread onto the SiO_2 surface and fuse to form a continuous bilayer[15,16] (step 2 in **Figures 1**, **Figure 2**, and **Figure 3**). The SUVs adsorption on the surface of the sensor is two-phasic and has a typical frequency minimum and maximum in the dissipation. A stable new frequency/dissipation baseline with a characteristic frequency shift (depending on the lipid composition) from 26 - 29 Hz (see **Table 1**) indicates a continuous bilayer on the surface.
5. When the SLB is stable (see step 3.4), equilibrate the system with the running buffer (10 mM HEPES, 150 mM NaCl, pH 7.4) at the required Ca^{2+} concentrations (ranging from 50 µM up to 1 mM $CaCl_2$, depending on the experiment) in an open flow mode for 40 min.
6. Add the protein (here, AnxA2) to the running buffer containing Ca^{2+} (see step 3.5). Perform the application of the protein in a loop-flow mode until an equilibrium steady state is reached (step 3 in **Figure 1**, **Figure 2**, and **Figure 3**).

NOTE: The protein concentration may range from 1 to 400 nM. Protein adsorption results in a concentration-dependent frequency shift reflecting the mass (protein) adsorption.

7. Dissociate the bound protein by chelating Ca^{2+} ions with 5 mM EGTA in the running buffer in open flow mode (step 4 in **Figures 1** and **Figure 2**).
   NOTE: A recovery of the frequency and dissipation to the SLB baseline indicates a total reversibility of protein binding. Association-dissociation cycles can be repeated to compare different concentrations or proteins.

4. Microbalance Cleaning

NOTE: Perform a minimal cleaning procedure after each measurement.

1. Regenerate the microbalance system with 50 mL of ddH_2O in a continuous open flow mode, remove the tubes from the water container, and let the system run dry.
2. Carefully remove the crystal sensor and clean it with the 2% SDS solution using the polytetrafluoroethylene holder (see step 2.1).
3. Dry the visible parts of the flow module interior where the sensor was placed.
   NOTE: Perform an intensive cleaning procedure after a series of 10 measurements.
4. Clean the system with a 2% SDS solution (50 mL) at 40 °C (setup in the software) in a continuous open flow (tube) mode, using a flow rate of 20 µL/min for extended contact with the detergent.
5. Clean with 250 mL of ddH_2O in continuous open flow mode at a flow rate of 160 µL/min.
   NOTE: After 4 months, carry out an extensive cleaning procedure according to the manufacturer's manual.

Representative Results

The decrease in the resonant frequency (Δf) correlates in a linear manner with the adsorbed mass (Δm), as defined by the Sauerbrey equation.[17]

$$\Delta f = -C_f \cdot \frac{\Delta m}{A}$$

Here, f is the resonant frequency, C_f is a constant that depends on the geometrical and physical characteristics of the given quartz and the resonant frequency, and A is the sensor surface area.

In most applications, the adsorbed layer is not completely rigid but viscoelastic. The resulting dampening of the quartz sensor oscillation is referred to as dissipation (D). The monitored dissipation changes (ΔD) correlate with the viscoelastic properties of the bound mass[18] and are defined as follows[8].

$$D = \frac{E_{dissipated}}{2\pi E_{stored}}$$

Here, $E_{dissipated}$ is the energy lost during one oscillation period, and E_{stored} is the total energy of the freely oscillating sensor.

To analyze and quantify the binding parameters, frequency isotherms are derived by plotting the equilibrium frequency shifts ($\Delta\Delta f_e$) against the protein concentrations. $\Delta\Delta f_e$ is defined as

$$\Delta\Delta f_e = [\,(\Delta f_{t2} - \Delta f_{t1})]$$

Here, Δf_{t1} represents the beginning of the protein adsorption and Δf_{t2} the equilibrium state. Nonlinear curve fitting can be performed by using a Hill expansion of the Langmuir equation as follows[6,8].

$$\Delta\Delta f_e = \Delta\Delta f_{max} \frac{[protein]^n}{(K_d)^n + [protein]^n}$$

Here, $\Delta\Delta f_{max}$ is the $\Delta\Delta f_e$ of the protein concentration resulting in maximum (saturating) binding, K_d is the apparent dissociation constant for the protein/membrane complex, and n is the Hill coefficient.

The Hill coefficient (n) describes the cooperativity of binding. For n = 1, the Hill adsorption model is a simple Langmuir isotherm (the equal binding sites and all molecules bind independently of each other to the lipid bilayer). If n ≠ 1, a bound ligand changes the membrane binding affinity for other ligands, either increasing (n > 1, positive cooperativity) or decreasing (n < 1, negative cooperativity) the affinity.

Figure 1 shows a schematic of the experimental workflow used in our laboratory to measure the shifts in resonance and frequency during Ca^{2+}-dependent binding and the release of AnxA2 to the lipid bilayer in the liquid phase. An exemplary recording is shown in **Figure 2**. **Figure 2A** shows the recording of the frequency curve and **Figure 2B** shows the dissipation shifts. The prominent drop in frequency upon the addition of the liposomes (**Figure 2A** [step 1]) indicates their adsorption. Because the buffer-filled vesicles are not rigid, but viscoelastic, the dissipation increases (**Figure 2B** [step 1]). Subsequently, the coalescing vesicles rupture. The concomitant release of the buffer inside the vesicles decreases the adsorbed mass until a stable plateau is reached (**Figure 2A** [step 2]). Of note, the addition of vesicles results in a high dissipation shift, while the shift in response to the bilayer is much smaller due to the rigid homogenous nature of the SLB (**Figure 2B** [step 2]). Step 3 in **Figure 2A** and **2B** records the binding of AnxA2 to the lipids, which adds mass, as seen by the clear frequency shift, but does not interfere with the bilayer structure, as indicated by the only small change in dissipation. When Ca^{2+} is removed by the chelating agent EGTA (**Figure 1** and **Figure 2** [step 4]), AnxA2 dissociates from the lipid film. The frequency, as well as the dissipation recordings, shift to the levels seen with the bilayer only (compare steps 2 and 4 in **Figure 2A** and **2B**), indicating that AnxA2 binding is totally dependent on Ca^{2+} and that the lipid film remains intact.

AnxA2, as do most of the annexins, depends on negatively charged lipids such as PS. This is clearly seen when POPS is absent in the lipid bilayer (**Figure 3**). **Figure 3A** shows the recording of the frequency curve and **Figure 3B** shows the dissipation shifts. Note that the frequency shifts to a stable baseline at -25 Hz, yet the dissipation is not altered (**Figure 3B** [step 2]), indicative of a proper bilayer formation. However, no changes in frequency (**Figure 3A**) or dissipation (**Figure 3B**) are observed after the addition of AnxA2 in the presence of Ca^{2+} (**Figure 3A** and **3B** [step 3]) or EGTA (**Figure 3A** and **3B** [step 4]), as AnxA2 cannot interact with the lipid film.

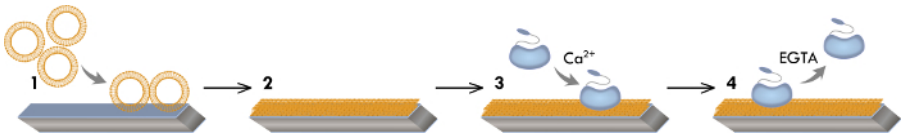

Figure 1: Graphical model of the experimental workflow. This workflow illustrates the vesicle absorption to the hydrophilic sensor surface (step 1), the vesicle fusion/rupture leading to the SLB formation (step 2), and the Ca^{2+}-dependent adsorption (step 3) and EGTA-dependent desorption of AnxA2 (step 4). Please click here to view a larger version of this figure.

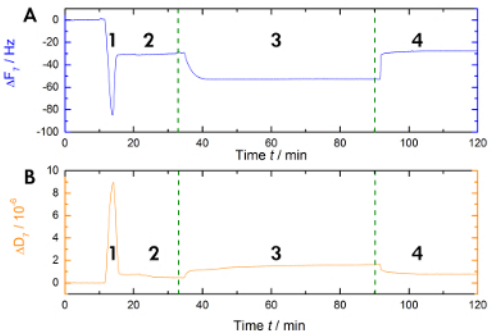

Figure 2: Exemplary recording. These panels show (**A**) the time-dependent monitoring of the 7th overtone resonance frequency and (**B**) the dissipation shifts of the quartz sensors during measurement. The application of the liposomes causes a rapid drop in the frequency baseline, whereas the dissipation baseline increases (step 1). The stabilization of the baselines indicates the formation of the bilayer (step 2). The AnxA2 (200 nM) adsorption (in the presence of Ca^{2+}) onto the POPS-containing lipid bilayer adds mass without significantly changing the dissipation, indicating that the lipid film is not perturbed (step 3). The recovery of the frequency baseline upon Ca^{2+} chelation with EGTA indicates the total desorption of the protein (step 4). Please click here to view a larger version of this figure.

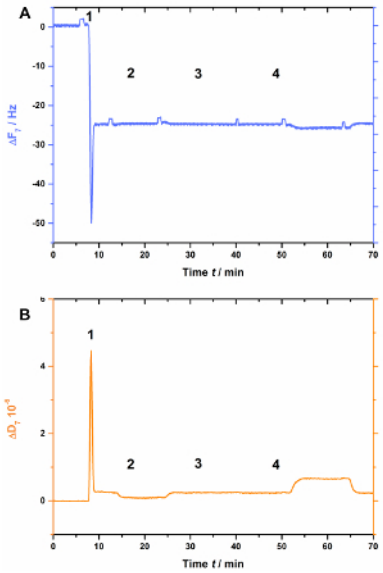

Figure 3: Negative control experiment, demonstrating that AnxA2 does not bind to SLBs in the absence of POPS. These panels show the addition of liposomes and the SLB formation (steps 1 and 2). No changes in (**A**) frequency or (**B**) dissipation are apparent after the addition of AnxA2 (step 3; 200 nM, in the presence of Ca^{2+}) or EGTA (step 4). Please click here to view a larger version of this figure.

Composition	ΔΔF/Hz after formation of SLBs	ΔΔD*10^{-6} after formation of SLB
POPC/POPS (80 : 20)	26.3 ± 0.2	0.26 ± 0.03
POPC/PI(4,5)P_2 (95 : 5)	26.5 ± 0.5	0.31 ± 0.02
POPC/POPS/Chol (60 : 20 : 20)	29.2 ± 0.2	0.45 ± 0.09
POPC/POPS/ PI(4,5)P_2/Chol (60 : 17 : 3 : 20)	29.6 ± 0.6	0.43 ± 0.10
POPC/DOPC/POPS/ PI(4,5)P_2/Chol (37 : 20 : 20 : 3 : 20)	29.4 ± 0.4	0.39 ± 0.14

Table 1: Lipid composition and formation data of the SLB[7].

Discussion

To answer questions concerning the structure-function relationship of cellular membranes both in a quantitative and qualitative manner, cell biology profits immensely from the use of biophysical approaches based on well-established and widely used techniques, including atomic force microscopy (AFM), surface plasmon resonance (SPR), and the QCM-D technique employed here. We showed in previous studies that annexin proteins bind in a Ca^{2+}-dependent manner to the immobilized membrane with high affinity. We use frequency and dissipation shifts of the 7th overtone (Δf7) because this represents the best compromise of detection sensitivity and oscillation stability.

This technique also permits a quantitative description of the membrane-protein interaction. AnxA2 binding to the membrane is characterized by positive cooperativity that is mediated by the conserved annexin core domain and depends on the presence of cholesterol. The quantitative data obtained for AnxA2 and AnxA8 are reported in detail elsewhere[6,8].

There are many critical steps in this protocol. Use the liposomes immediately; otherwise, small vesicles might fuse into bigger vesicles with less surface tension, leading to the inhibition of the lipid bilayer formation. Maintain a constant temperature during the measurements. Each small deviation in temperature results in a not negligible frequency and dissipation shift. Avoid air bubbles; otherwise, the system is unstable and will not establish a baseline.

The Sauerbrey equation allows the direct conversion of the observed frequency changes into changes in mass and is, therefore, widely used. However, the assumption of a linear correlation between the change in resonance frequency and the added mass only holds true for components forming a rigid and uniform film on the sensor surface. The Sauerbrey equation cannot be used for viscoelastic adsorbents such as water-rich protein films, lipid layers with incorporated water, or even adsorbed cells. Here, more complex mathematical models are required. Therefore, it is extremely important to simultaneously monitor the changes in frequency and dissipation. To detect structural changes during the measurement, ΔD *versus* Δf ratios can be plotted, with a straight line indicating no conformational changes.

A major advantage of this technique is the possibility to use a very broad range of materials as substrates. Moreover, it is a reliable and direct method to study a broad range of macromolecular interactions, as the proper formation of the surface-coating films (such as SLB), as well as further protein-lipid interactions, can be monitored online.

This protocol can be applied to other membrane-interacting proteins, for example, BAR domain proteins[19], the ERM (ezrin, radixin, and moesin) protein family that has an important role in membrane-cytoskeleton linkage[20,21,22], or proteins containing C2 or PH domains. Moreover, a wide range of applications of this technique to study biological materials has been successfully published, thus establishing QCM as a well-suited experimental platform to study the interactions of more complex macromolecular assemblies or even cells[23,24].

Disclosures

The authors have nothing to disclose.

Acknowledgements

This work was supported by the Deutsche Forschungsgemeinschaft under grants SFB 858/B04, EXC 1003, SFB 1348/A04, and SFB 1348/A11.

References

1. Simons, K., Toomre, D. Lipid rafts and signal transduction. *Nature Reviews Molecular Cell Biology.* **1** (1), 31-41 (2000).
2. Gerke, V., Creutz, C. E., Moss, S. E. Annexins: linking Ca^{2+} signalling to membrane dynamics. *Nature Reviews Molecular Cell Biology.* **6**, 449-461 (2005).
3. Mim, C., Unger, V. M. Membrane curvature and its generation by BAR proteins. *Trends in Biochemical Science.* **37**, 526-533 (2012).
4. Rescher, U., Ruhe, D., Ludwig, C., Zobiack, N., Gerke, V. Annexin 2 is a phosphatidylinositol (4,5)-bisphosphate binding protein recruited to actin assembly sites at cellular membranes. *Journal of Cell Science.* **117**, 3473-3480 (2004).
5. Gerke, V., Moss, S. E. Annexins: from structure to function. *Physiological Reviews.* **82**, 331-371 (2002).
6. Heitzig, N. *et al.* Cooperative binding promotes demand-driven recruitment of AnxA8 to cholesterol-containing membranes. *Biochimica et Biophysica Acta (BBA) - Molecular and Cell Biology of Lipids.* **1863** (4), 349-358 (2018).
7. Drücker P., Grill, D., Gerke, V., Galla, H. J. Formation and characterization of supported lipid bilayers containing phosphatidylinositol-4,5-biphosphate and cholesterol as functional surfaces. *Langmuir.* **30**, 14877-14886 (2014).
8. McConnell, H. M., Watts, T. H., Weis, M. R., Brian, A. A., Supported planar membranes in studies of cell-cell recognition in the immune system. *Biochimica et Biophysica Acta - Reviews on Biomembranes.* **864**, 95-106 (1986).
9. Anderson, T. H. *et al.* Formation of supported bilayers on silica substrates. *Langmuir.* **25**, 6997-7005 (2009).
10. Pfeiffer, L., Petronis, S., Koper, I., Kasemo, B., Zach, M. Vesicle adsorption and phospholipid bilayer formation on topographically and chemically nanostructured surfaces. *Journal of Physical Chemistry B.* **114**, 4623-4631 (2010).
11. Cho, N. J., Jackman, J. A., Liu, M., Frank, C. W. pH-Driven assembly of various supported lipid platforms: a comparative study on silicon oxide and titanium oxide. *Langmuir.* **27**, 3739-3748 (2011).
12. Jackman, J. A., Tabaei, S. R., Zhao, Z., Yorulmaz, S., Cho, N. J. Self-Assembly formation of lipid bilayer coatings on bare aluminium oxide: overcoming the force of interfacial water. *ACS Applied Materials & Interfaces.* **7**, 959-968 (2015).
13. Olson, F., Hunt, C. A., Szoka, F. C., Vail, W. J., Papahadjopoulos, D. Preparation of liposomes of defined size distribution by extrusion through polycarbonate membranes. *Biochimica et Biophysica Acta(BBA) - Biomembranes.* **557** (1), 9-23 (1979).
14. Richter, R., Mukhopadhyay, A., Brisson, A. Pathways of lipid vesicle deposition on solid surfaces: a combined QCM-D and AFM study. *Biophysical Journal.* **85** (5), 3035-3047 (2003).
15. Richter, R. P., Bérat, R., Brisson, A. R. Formation of solid-supported lipid bilayers: an integrated view. *Langmuir.* **22** (8), 3497-3505 (2006).
16. Sauerbrey, G. Verwendung von Schwingquarzen zur Wägung dünner Schichten und zur Mikrowägung. *Zeitschrift für Physik A Hadrons and Nuclei.* **155** (2), 206-222 (1959).
17. Rodahl, M., Höök, F., Krozer, A., Brzezinski, P., Kasemo, B. Quartz crystal microbalance setup for frequency and Q-factor measurements in gaseous and liquid environments. *Review of Scientific Instruments.* **66** (7), 3924-3930 (1995).
18. Drücker, P., Pejic, M., Grill, D., Galla, H. J., Gerke, V. Cooperative binding of annexin A2 to cholesterol-and phosphatidylinositol-4, 5-bisphosphate-containing bilayers. *Biophysical Journal.* **107** (9), 2070-2081 (2014).
19. Galic, M. *et al.* External push and internal pull forces recruit curvature-sensing N-BAR domain proteins to the plasma membrane. *Nature Cell Biology.* **14** (8), 874-881 (2012).
20. Fehon, R. G., McClatchey, A. I., Bretscher, A. Organizing the cell cortex: the role of ERM proteins. *Nature Reviews Molecular Cell Biology.* **11** (4), 276-287 (2010).
21. Braunger, J. A., Kramer, C., Morick, D., Steinem, C. Solid supported membranes doped with PIP2: influence of ionic strength and pH on bilayer formation and membrane organization. *Langmuir.* **29** (46), 14204-14213 (2013).
22. Bianco, M. *et al.* Quartz crystal microbalance as cell-based biosensor to detect and study cytoskeletal alterations and dynamics. *Biotechnology Journal.* 1700699 (2018).
23. Chen, J. Y., Penn, L. S., Xi, J. Quartz crystal microbalance: Sensing cell-substrate adhesion and beyond. *Biosensors and Bioelectronics.* **99**, 593-602 (2018).
24. Bragazzi, N. L. *et al.* Quartz-Crystal Microbalance (QCM) for Public Health: An Overview of Its Applications. In *Advances in Protein Chemistry and Structural Biology.* Edited by Donev, R., **101**, 149-211, *Academic Press.* (2015).